

Preparation and Characterization of $ZnO_{99.5-x}NiO_{0.5}$. CuO_x Ceramics

Osama A. Desouky

Bilbis Higher Institute of Engineering (BHIE), Bilbis, Sharqia ,Egypt

Abstract: *The microstructure and (I –V) characteristics of bodies in the system $ZnO_{99.5-x}NiO_{0.5}CuO_x$ where x lie between 0.3 to 6 mol% and sintered at 1100°C were verified. The microstructure revealed the presence of ZnO grains embedded in a glassy matrix mainly formed of CuO. The incorporation of CuO reduced the abnormal grain growth of ZnO and improved the nonlinear property of the bodies. Highest coefficient of non-linearity was obtained by the addition of 4.0 mol% CuO, with a value of 115.6.*

Keywords: ZnO-NiO-CuO- Ceramics- Resistivity- dielectric constant

1. Introduction

ZnO-based varistors are important technological materials found their application as surge arresters in high power electrical systems and electronic circuits [1]. Electrical properties of ZnO – ceramics directly depend on the composition and micro structural characteristics; such as grain size, density and the distribution of the different phases. Matsuoka [1] developed a multi-component ZnO-based varistor composition. The presence of Bi_2O_3 , play a role in the densification of the product through a reactive liquid-phase sintering [2–6]. Moreover, an improvement in the coefficient of nonlinearity coefficients and smaller leakage currents was achieved by the addition of 1 wt. % glass frit to Matsuoka's composition [7]. Substituting the Bi_2O_3 by further addition of 10 wt.% glass improved the processing parameters and enhanced electrical stability [8–13]. Many studies have been conducted on enhancing the sintering of ZnO and improving the coefficient of non-linearity through the incorporation of dopants; such as Bi_2O_3 - ZnO [14-16], Sb_2O_3 - ZnO [17], Al_2O_3 -ZnO [18], PbO- ZnO [19], CuO- ZnO [20], and SiO_2 - ZnO [21]. Microstructural homogeneity are the most significant and governing parameters in ceramic processing [25]. The nonlinear current density –electric field (J-E) characteristic are expressed by $(J = KE^\alpha)$, where K is a constant and α is the nonlinear coefficient. [22-24]. The ZnO grain size governs the breakdown voltage. Sb_2O_3 is commonly used as a grain growth inhibitor for Bi_2O_3 -doped ZnO varistors [26]. Whereas the band gap of ZnO decreased by increase in the calcination temperature. Also, the absorption maximum is also shifted to higher wavelengths as has been reported by Kumar et al. [27].

Copper oxide is a transition-metal oxide with a monoclinic structure [33, 34]. It is a covalent semiconductor having an indirect band gap between 1.2eV and 1.5eV. It is applied in several industrial applications; like solar energy storage, semiconductors and catalysis. In this work, the effect of Copper (II) oxide addition on the physical properties, microstructure and (I –V) characteristics of ; $ZnO_{99.5-x}$. $NiO_{0.5}$. CuO_x ceramics sintered at 1100°C are verified.

2. Experimental Procedure

High purity oxide powder starting precursors were mixed as given in Table. 1. mix Nopresents the pure ZnO alone. The other seven mixes contain CuO in ascending proportion between 0.3 to 6 mole % based on the formula $ZnO_{99.5-x}$. $NiO_{0.5}$. CuO_x . Powders were thoroughly wet mixed for 4 h in a ball mill using alumina balls and deionized water. The mixtures were then dried, pressed into discs specimens with the following dimensions, diameter either 1.2 cm or 5 cm and thickness 0.3 cm were processed under a force of 70kN, dried and sintered at 1100 °C / 2 hours with a heating rate of 100 °C/ h and a cooling rate at 200 °C/ h .The phases developed during firing were identified by XRD utilizing an equipment; Philips type 1700, copper radiation and a Ni filter. Microstructure developed was examined under SEM type Philips XL 30 provided with EDS after sputtering the surface with gold. The surface morphology was investigated by the atomic force microscopy (AFM, Bruker Dimension Icon) using the Peak Force Tapping and silicon nitride probes with sharp tips (a tip radius: 2 nm).The bulk densities of the sample were calculated from their weight and dimensions. For electrical measurements, the as-sintered specimens were lapped on both surfaces to ensure flat and parallel surfaces. They were coated with conductive silver paint on both surfaces, and then heat cured to provide ohmic contacts. The current–voltage (I–V) characteristics were determined at room temperature using a variable dc power supply.

3. Results and Discussion

The density of ceramic bodies within the composition: $ZnO_{99.5-x}$. $NiO_{0.5}$. CuO_x increased from 5.24 to 8.82 g cm⁻³ as shown in Table .1. The addition of CuO results in an increase in the bulk density values of the specimens at 1100 °C/2h attributed to the difference in the densities of ZnO, NiO and CuO. (TD=5.78, 6.67& 6.2 g cm⁻³ in ZnO , NiO , & CuO respectively).

XRD of sintered samples reveal no change in the existing oxide phases. It is evident that the main peaks present correspond to the contributing oxides mainly ZnO, yet some peaks were absent that might be related to a preferred orientation. But, no reaction took place between ZnO and CuO. The absence of the corresponding diffraction lines of

CuO and NiO in the mixes is explained through the complete dissolution of these dopant oxides in the lattice of ZnO forming a limited solid solution. Therefore, a change in the lattice constants of the ZnO was recorded depending on the affinity to a particular ion and on the overall mix composition. Mixes fired at 1100 °C for 2 hours, showed a shift in the d – spacing equivalent to (0.02 – 0.04 Å) in the main ZnO peak, indicating a kind of limited solid solution of CuO in the oxide. A maximum shift of 0.04 Å was recorded for mix containing 6 mol % CuO.

SEM micrographs of the fired samples containing different Cu contents are shown in Figs.1 and 2. ZnO grains forming the dark part interconnected with light colored liquid phase constituting the grain boundaries as was previously described in ref [35-37]. Nodes occur either at triple points or occasionally within the grains. SEM of mix N₁ formed of ZnO_{99.2} CuO_{0.3} and NiO_{0.5} present in Fig.2, shows crystal growth of ZnO denoted by annular epitaxial tiny ex-solution of Ni- rich phase, lying inter-granular and along the growth rings. SEM of mix N₆ having the composition ZnO_{95.5} CuO_{4.0} and NiO_{0.5} shows two phases : ZnO grains and inter-granular liquid phase composed of the three components ZnO, NiO and CuO solid solution accumulating at triple points and surrounding grain boundaries (light colour).

Figs(3-5) show the AFM plane image for sample N0 at both firing temperature 900°C to 1100°C scan range for a single scan is 5µm x 5µm and 10 µm x 10 µm respectively which represent the hexagonal crystalline shape of ZnO. The ZnO grains exhibit different, but homogeneous levels, which allow distinguishing individual grains. Fig.4. shows the three dimensional image for N0 also for the two firing temperature with heights from 0 nm at the darkest places and maximum height of about 960 nm and 1.15µm at the brightest places respectively. Fig.5. shows their particles analyses which are maximum diameter, mean radius, perimeter, surface area, volume, distortion and roughness for each particle. . This data represent that the average of mean radius of N0 grains fired at 900°C was 0.43 µm and average surface roughness of 1.6 and that of N0 fired at 1100°C was 0.52 µm and surface roughness of 1.7. That is mean that there are increase in the grain size by increasing firing temperature and increasing in the total surface roughness. AFM results of samples N2 and N6 are shown in Figs (6–11) respectively at both firing temperature 900°C to 1100°C with the same scan range. The images shows that the grains have larger size for sample N2 with 0.5mol% of CuO and 0.5mol% NiO where fired at 1100°C, there is a decrease in the grain size of the particles of mix N6 containing the maximum CuO addition. The 3D difference between samples surfaces represented in three dimensional images of the group in Figs. (6, 7) and Table.2. This is clearly demonstrated in Figs.(8 -11) and Table.2. The average difference increased with the content of dopant in bodies fired at low temperature and drops at high ones.

The (V-I) Characteristics were measured at voltage between (0-5) KV and current between 0-10 mA. The relation between I and V for the different mixes is shown in Fig.12. The different mixes clearly show a non-linear behaviour as evident from the calculated values of the coefficient of non-linearity in table 1. The CuO added showed an increase in

these values up to 4 mol%, that decreases with higher contents. The characteristic curves of different mixes are greatly divided into two regions; a pre-breakdown at low voltage region and an off- state and nonlinear properties as an on-state high voltage region, the sharper the knee of the curves between the two regions, the better the non-linearity. The presence of 0.5 mol% NiO with (ZnO+ CuO) increased the coefficient to 115. Some properties of added CuO and (ZnO-0.5NiO) Varistor are present in Table .1. Densification occurs via the formation of a ZnO- NiO- CuO eutectic liquid occurring on heating and cooling depending on composition and sintering temperature. The grain size of ZnO is controlled by this second phase. CuO improved densification by minimizing the amount of closed pores. Whereas the role played by the NiO increases was felt in the grain growth of ZnO forming clusters. NiO and CuO went into a limited solid solution with the ZnO as evident from the shift in the d-spacing, causing some of the ZnO to ex-solute accumulating at the triple point reaching its maximum in mix (N₆). Microstructure of ZnO ceramics plays an important role in the electric characteristic displayed. There are two models postulated to describe the microstructure of ZnO depending on the constitution. The presence of a liquid phase facilitated the sintering process and developed atomically interfaces, uniform intergranular phase required for non-linear conduction. Asokan [28] reported that the non-linearity coefficient in the binary system ZnO- Bi₂O₃ lies between 2 to 6. The large value = 40 obtained in the commercial varistors is achieved by different dopants added. Bi₂O₃ and Pr₆O₁₁ are the key intergranular components which impart the non-ohmic properties. The copper oxides do not react with ZnO to form a compound, whereas in the binary system between ZnO- Nb₂O₃, the following compound Zn₃Nb₂O₈ was recorded by Asokan [28]. Kutty and Raghu [29] show that sintered polycrystalline ZnO ceramics with copper as the only additive exhibited nonlinear V- I relations. Cu is well known as an acceptor in II- IV compounds, with an ionic radius of 0.62 Å for Cu⁺², which is comparable to that of Zn⁺²(0.68 Å). It is argued that Cu acceptors are compensated by holes in the grain boundary layers. Whereas, the concentration of intrinsic donors is higher in the grain interior. The presence of the positive charges leads to thinning of the depletion region, which results in non-ohmic behavior and the non-ohmic breakdown behavior of ZnO ceramics is caused by hole creation in ZnO [30-32]. The variation of dielectric constant as function of temperature in the range between 300 to 523 K is shown in Fig .13. Low and high additions 0.3 and 6 mol % CuO show increased dielectric constant in the range of temperature experimented. Fig .14 . shows the relation between conductivity (Ω.m), and temperature at constant frequency (10 KHz), for different mixes, increasing the concentration of CuO in mixes (N₂-N₆) leads to a gradual increase of σ as a function of temperature, due to the fact that, the increase of temperature activates the mobility of ions and increase the carrier density. This in turn increases the conductivity values was affected by the content of copper oxide added. Thus, it increases up to 4 mol % addition then decreased on 6 mol % addition. This may be explained in the light of the microstructure developed formed of semi-conductive ZnO grains surrounded by an insulating glassy phase which is similar to that of grain boundary layer capacitors as a result the observed dielectric

constant and conductivity increased with increase in copper oxide.

4. Conclusions

The results obtained for the studied range of mixes in the composition $ZnO_{99.5-x}NiO_{0.5} \cdot CuO_x$ the following conclusions are reached:

- Non-ohmic behaviour was obtained for polycrystalline ZnO with copper as the only additive.
- The nonlinear coefficient increases as the amount of CuO additive is increased.
- A highest nonlinear coefficient of 115.6 was obtained for the sample containing 4 mol% CuO in 0.5 mol% NiO doped ZnO varistor.
- Crystal growth of ZnO represented by annular epitaxial tiny exsolution of Ni- rich phase, lying intergranular and along the growth rings.

Further work in this field is carried to cover the addition of copper oxide in the presence of other additives.

References

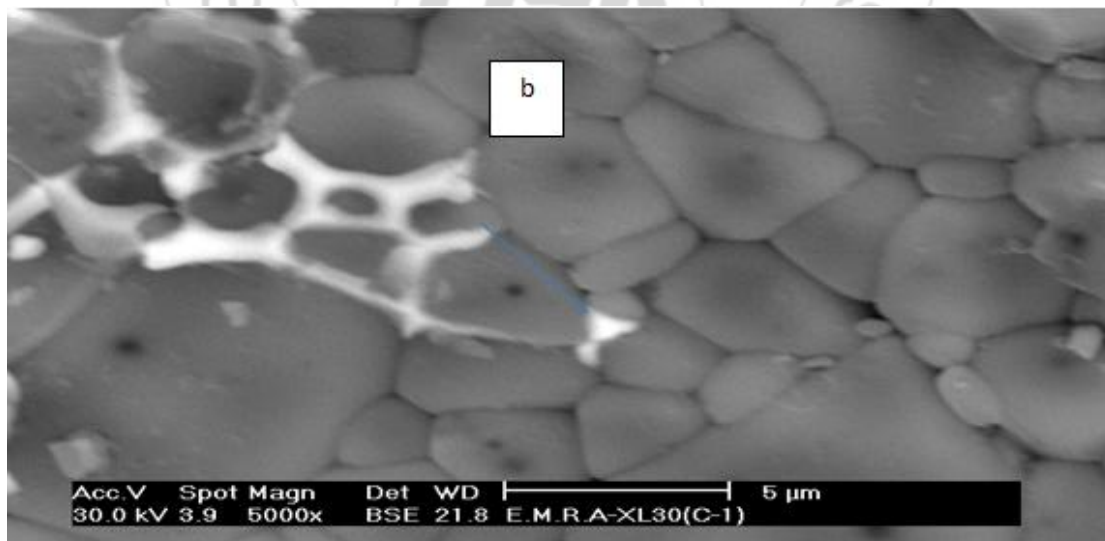
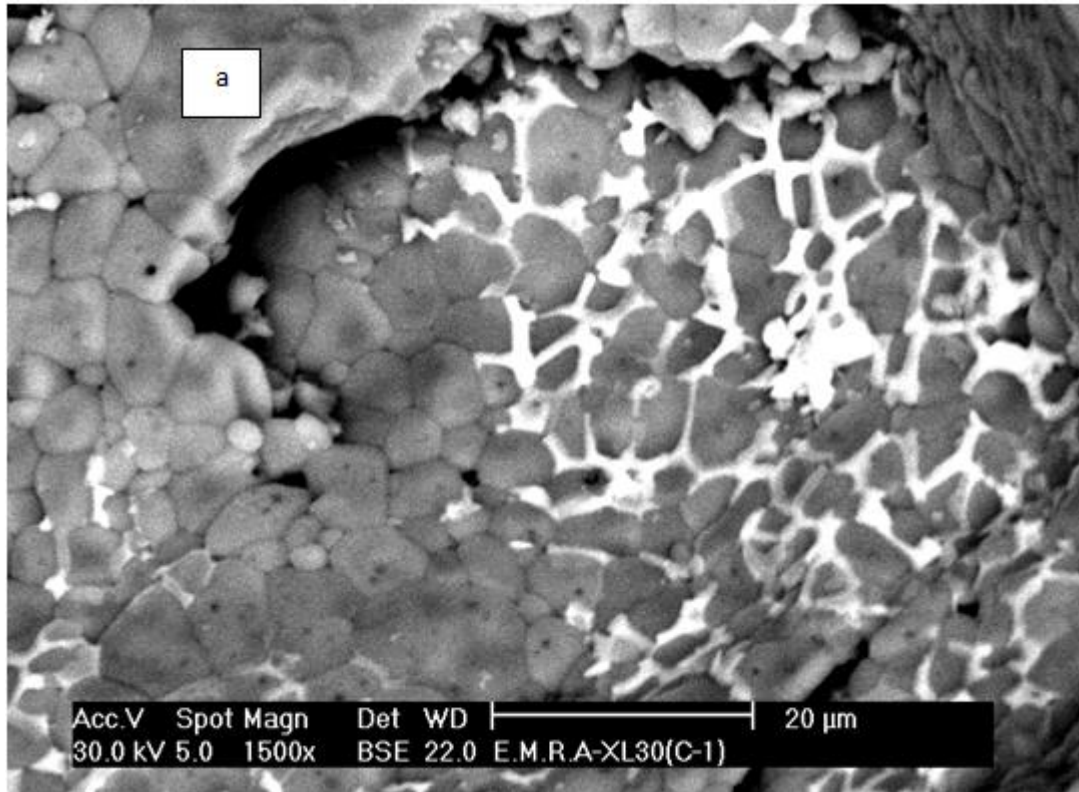
[1] M. Matsuoka, Jpn. J. Appl. Phys. 10 ,(1971) 736.
 [2] L.M. Levinson, H.R. Phillipp, Am. Ceram. Soc. Bull. 65 (1986) 639.
 [3] R. Einzinger, Annu. Rev. Mater. Sci. 17 (1987)299 .
 [4] K. Eda, IEEE Elec. Insul. Mag. 5,(1989) 28.
 [5] T.K. Gupta, J. Am. Ceram. Soc. 73,(1990) 1817.
 [6] D.R. Clarke, J. Am. Ceram. Soc. 82 ,(1999) 485.
 [7] N. Shohata, J. Yoshida, Jpn. J. Appl. Phys. 16 ,(1977) 2299.
 [8] B.-S. Chiou, F.W. Jih, Br. Ceram. Trans. J. 85 ,(1986) 118.
 [9] Y.-S. Lee, T.-Y. Tseng, J. Am. Ceram. Soc. 75 ,(1992) 1636.
 [10] Y.-S. Lee, T.-Y. Tseng, J. Mater. Sci., Mater.Electron. 6,(1995) 90.
 [11] Y.-P. Wang, W.-I.Lee, T.-Y. Tseng, Appl. Phys. Lett. 69,(1996) 1807.
 [12] Y.-S. Lee, T.-Y. Tseng, J. Mater. Sci., Mater.Electron.8 ,(1997) 115.
 [13] Y.-S. Lee, T.-Y. Tseng, J. Mater. Sci., Mater.Electron.9 (1998) 65.
 [14] T. Senda and R.C. Bradt., J. American Ceram .Soc., 73 (1), (1990) 106.
 [15] D.Dey and R.C Bradt ., J. American Ceram . Soc., 75 (9), (1992)2529.
 [16] G. Willam .Morris ., J. American Ceram . Soc., 56 (7) (1973), 360.
 [17] T.Senda T.and Bradt R.C ., J. American Ceram . Soc., 74 (6),(1991) 1296.
 [18] P.Q. Mantas ,Hanj., and A.M.R .Senos., J. Mater, Res., 16(2),(2002) 459.
 [19] H.O .Toplan.,H.Erkalfa and O.T .Ozkan., Ceramics – Silikaty,74 (3)(2003)116.
 [20] F .Apaydin.,O. Toplan .and Yildizk., J.Mater .Sci., 40 (3), (2005) 677.
 [21] T. Asokan, G.N.K. Iyengar and G.R.N.Bushana., Br. Ceram. Trans. (86),(1987) 190.
 [22] R.K. Sendi, A. Munshi, S. Mahmud, Superlattices and Microstructures 69, (2014) 212.
 [23] C. -W. Nahm, Ceramics International 39, (2013) 3417.
 [24] H. Zhou, R. Guo, D. Chu, B. Chang, Y. Qin, L. Fang, Journal of Materials Science: Materials in Electronics 24, (2013) 4987.
 [25] M.Takada,S.Yashikado,Jornal of European ceramic society 39,(2010) 531.
 [26] T.K. Gupta, Applications of zinc oxide varistors, J. Am. Ceram. Soc. 73,(1990) 1817.
 [27] S.S.Kumar,P.V.Warlu,V.R.RaO and G.N.RaO ; International nano letters licensee Springer (2013).
 [28] T. Asokan.Br. Ceram.Trans. J., 86,(1987) 87.
 [29] T.R.N. Kutty and N.Ragha , Appl. Phys. Lett., 19,(1989) 5512.
 [30] G.Blatter and F.Greuter , phys. Rev.B. 12,(1986) 8555.
 [31] G.E.Prke , S.R,Kuttz and P.L. Gourley , J.Appl. phys. 12,(1985) 5012.
 [32] G.D.Mahan, L.M.Levinson and H.R.Philipp, J.Appl. phys.4, (1979) 2799.
 [33] Shanid, M. N. A., Khadar, M. A, Thin Solid Films **516**, (2008)6245.
 [34] Wang, H., Jin-Zhong, X., Jun-Jie, Z., Hong-Yuan, C., Journal of Crystal Growth 244, (2002) 88.
 [35] K. Mukae, Am. Ceram. Bull., **66**, (1987) 1329.
 [36] Y. S. Lee, K. S. Liao, and T.-Y. Tseng, J. Am. Ceram. Soc., **79**,(1996) 2379.
 [37] C. W. Nahm, Mater. Lett.,**47**, (2001) 182.

Table 1: Summary of sample composition, Shrinkage% ,relative density % and nonlinearity coefficient for different ZnO–NiO–CuO ceramics

Mixes/Oxides	ZnO mol%	NiO mol%	CuO mol%	Shrinkage %	Relative density%	Nonlinearity coefficient	Break down voltage
N0	100	-	0	18.4	5.24	13.56	5100
N1	99.2	0.5	0.3	18.5	6.41	69.8	5190
N2	99	0.5	0.5	21.5	6.82	73.2	5240
N3	98.5	0.5	1	24.3	6.96	80.4	5250
N4	97.5	0.5	2	25.1	6.35	88.9	5110
N5	96.5	0.5	3	26.2	6.72	100.2	5200
N6	95.5	0.5	4	27.1	6.81	115.6	5060
N7	94.5	0.5	5	29.4	8.32	104.1	4200
N8	93.5	0.5	6	30	8.96	69.3	4160

Table 2: Average mean radius and average surface roughness for some mixes

Sample name	Mean Radius (μm)	Roughness
N0 900	0.43	1.6
N0 1100	0.52	1.7
N2 900	0.28	1.55
N2 1100	0.46	1.81
N6 900	0.45	1.81
N6 1100	0.36	1.77



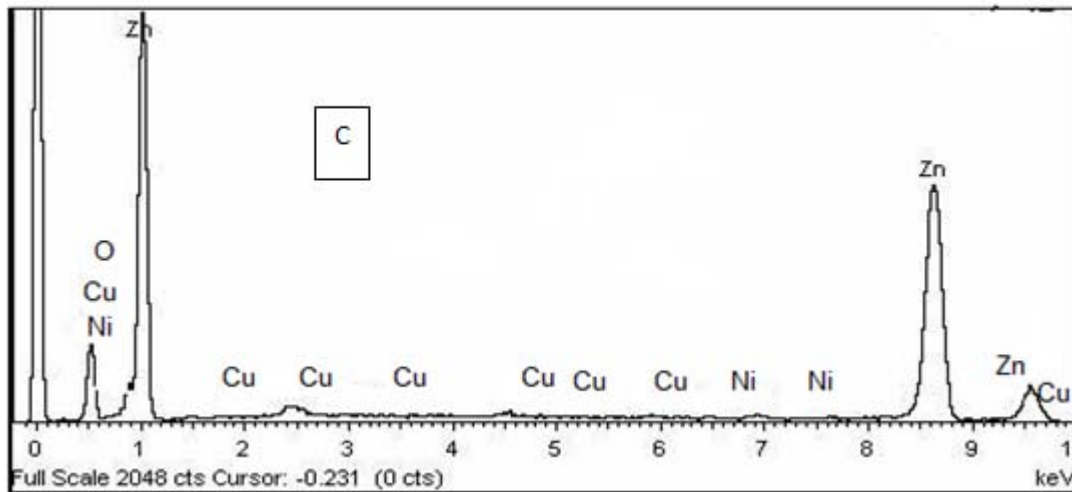


Figure 1: SEM of Mix N1. (a) Thermally etched, showed two phases ZnO grains and intergranular phase at triple point. X= 1500 (b) Thermally etched, growth of ZnO grains in preferred orientation. Exsolution of (Ni) rich phase along the grains and intergranular (c)EDS show the distribution of CuO, and NiOwith ZnO and CuOintergranular accumulation.

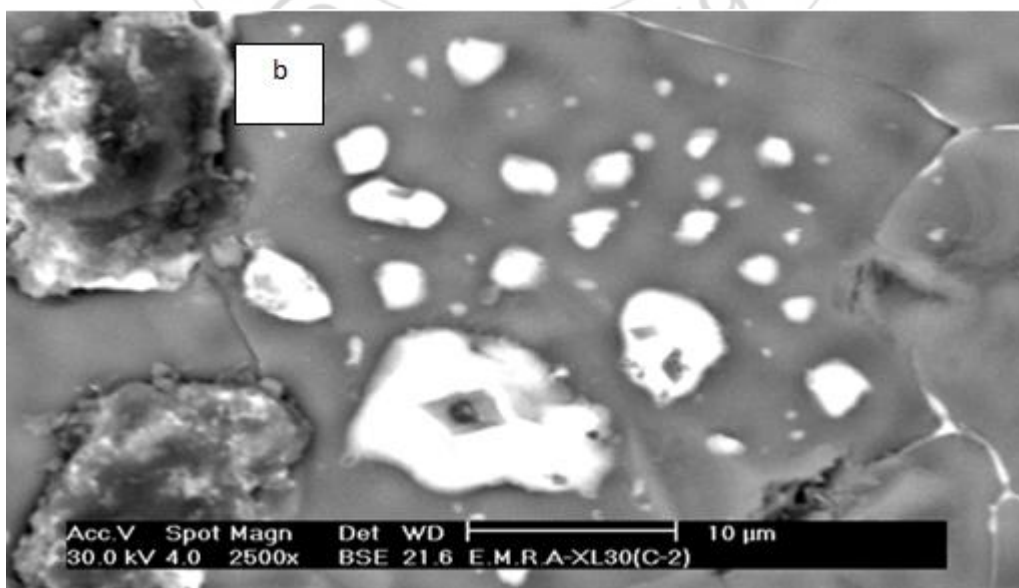
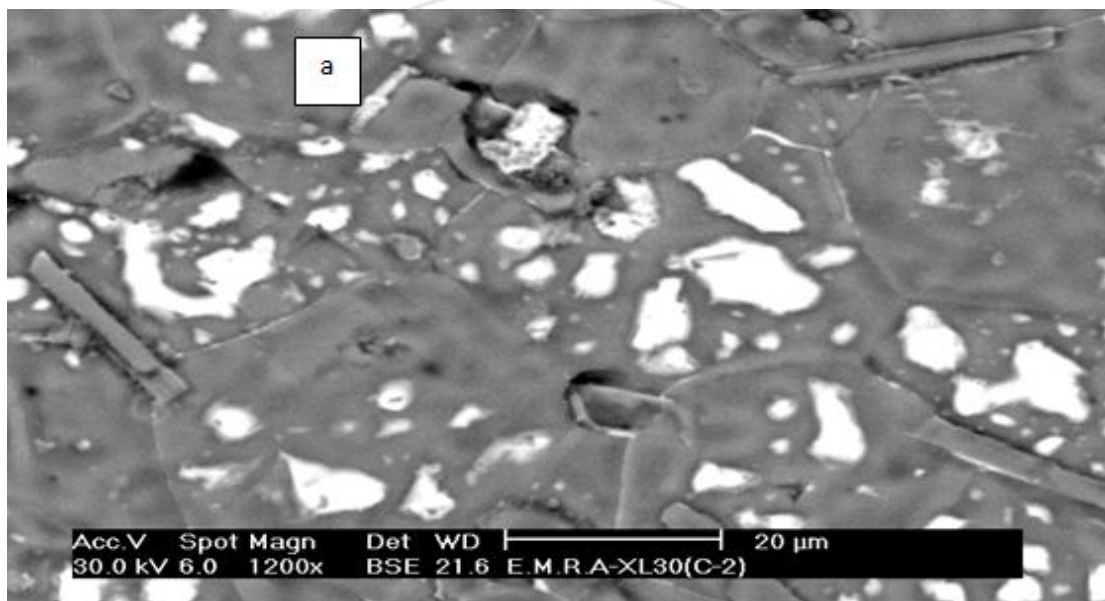


Figure 2: SEM of mix N6. (a)Thermally etched, Shows different grains, randomly oriented, X=1200 (b) Thermally etched, shows two phases ZnO grains and intergranular phase at triple point, Zn is exsoluting accumulating at grain boundaries (white colour), grain growth is evident. X= 2500.

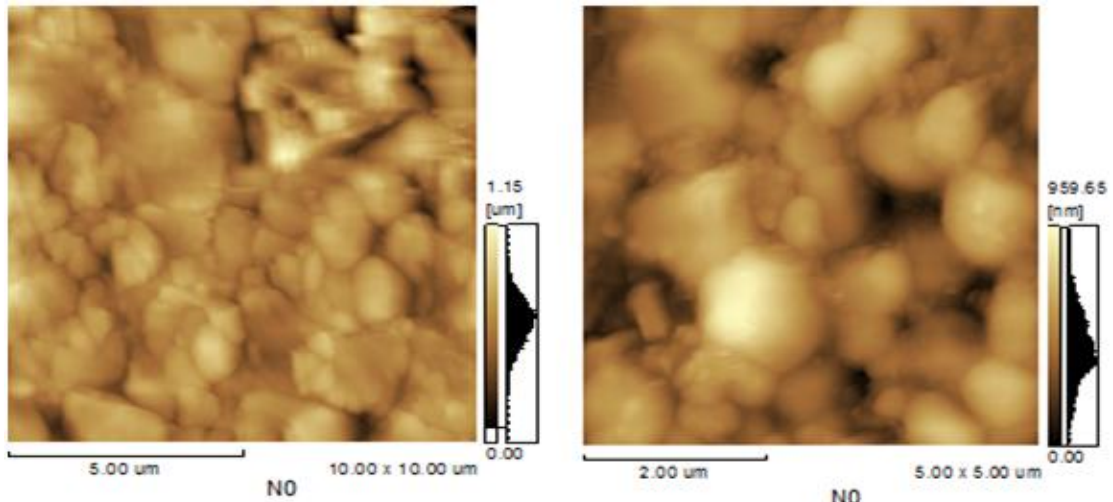


Figure 3: AFM plane image for sample N0/900°C & 1100°C.

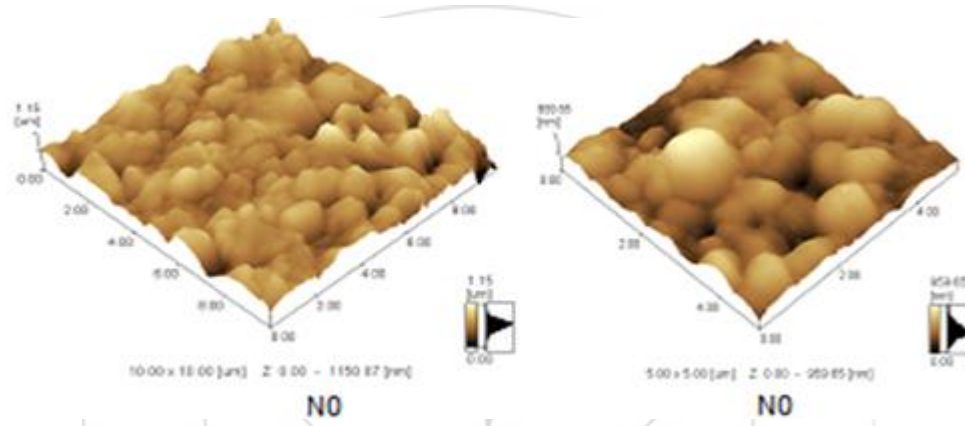


Figure 4: AFM 3D image for sample N0/900°C & 1100°C.

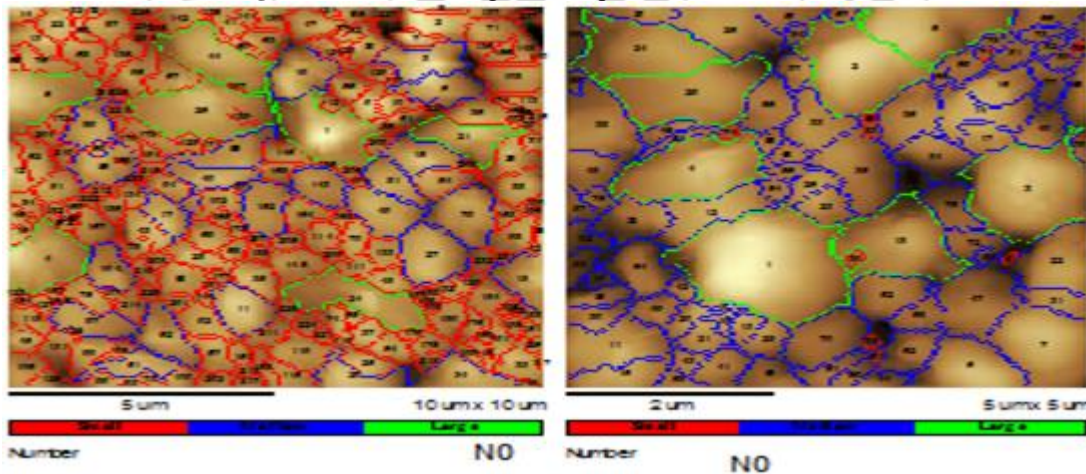


Figure 5: AFM particle analyses image for sample N0/900°C & 1100°C

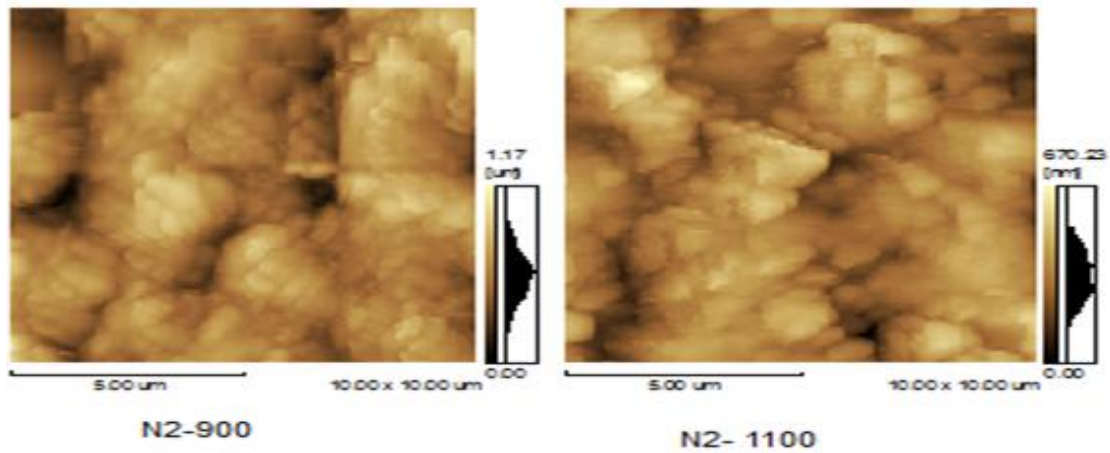


Figure 6: AFM plane image for sample N2/900°C & 1100°C.

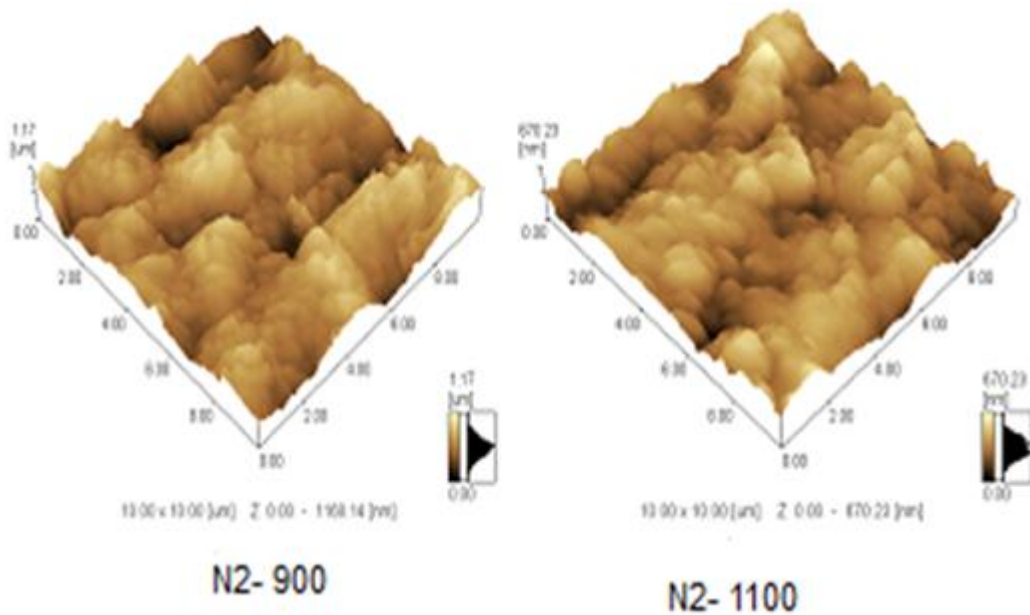


Figure 7: AFM 3D image for sample N2/900°C & 1100°C.

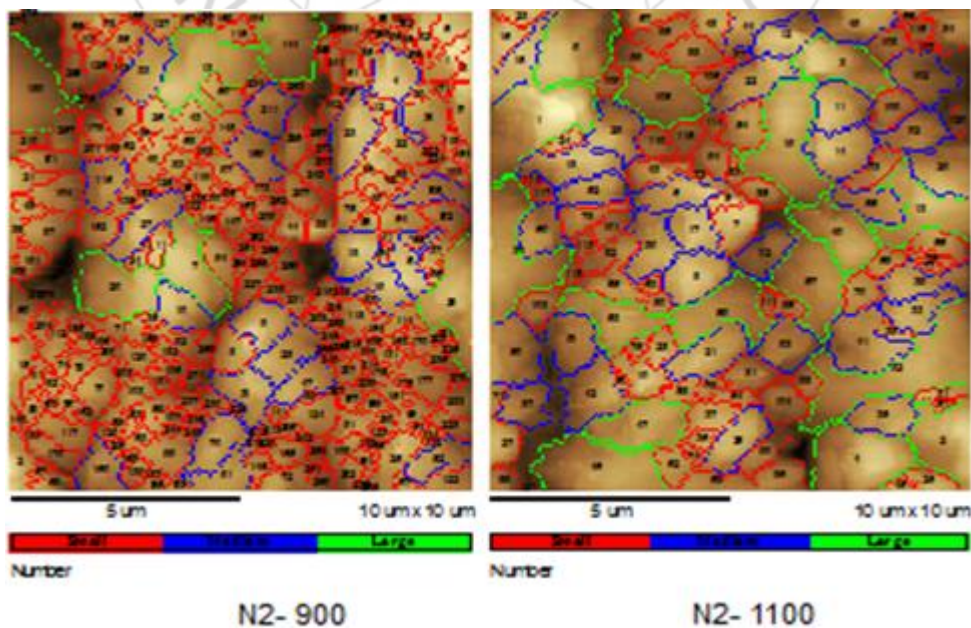


Figure 8: AFM particle analyses image for sample N2/900°C & 1100°C.

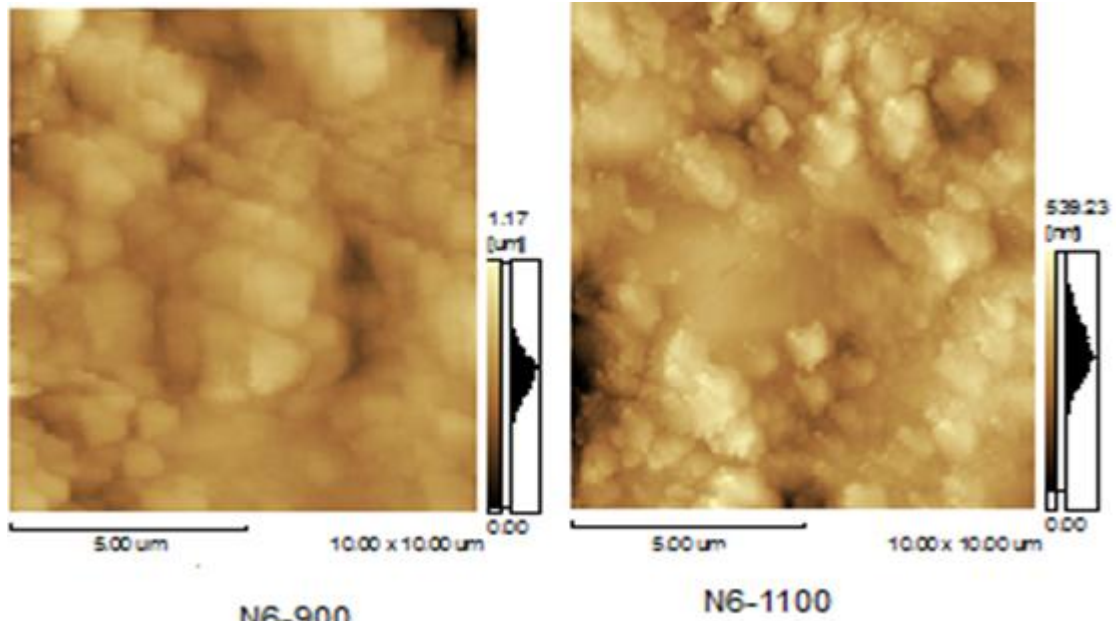


Figure 9: AFM plane image for sample N6/900°C & 1100°C.

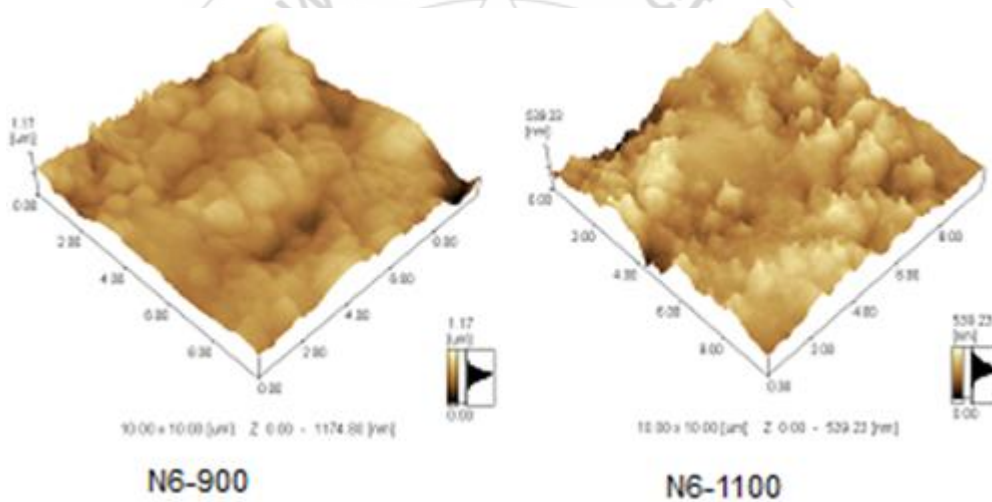


Figure 10: AFM 3D image for sample Z6/900°C & 1100°C

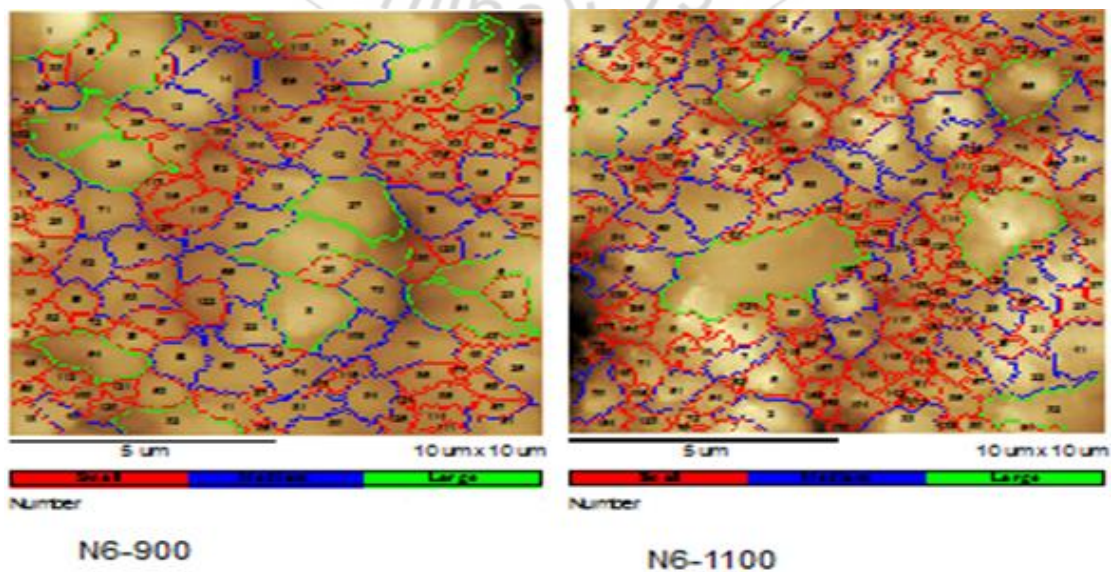


Figure 11: AFM particle analyses image for sample N6/900°C & 1100°C.

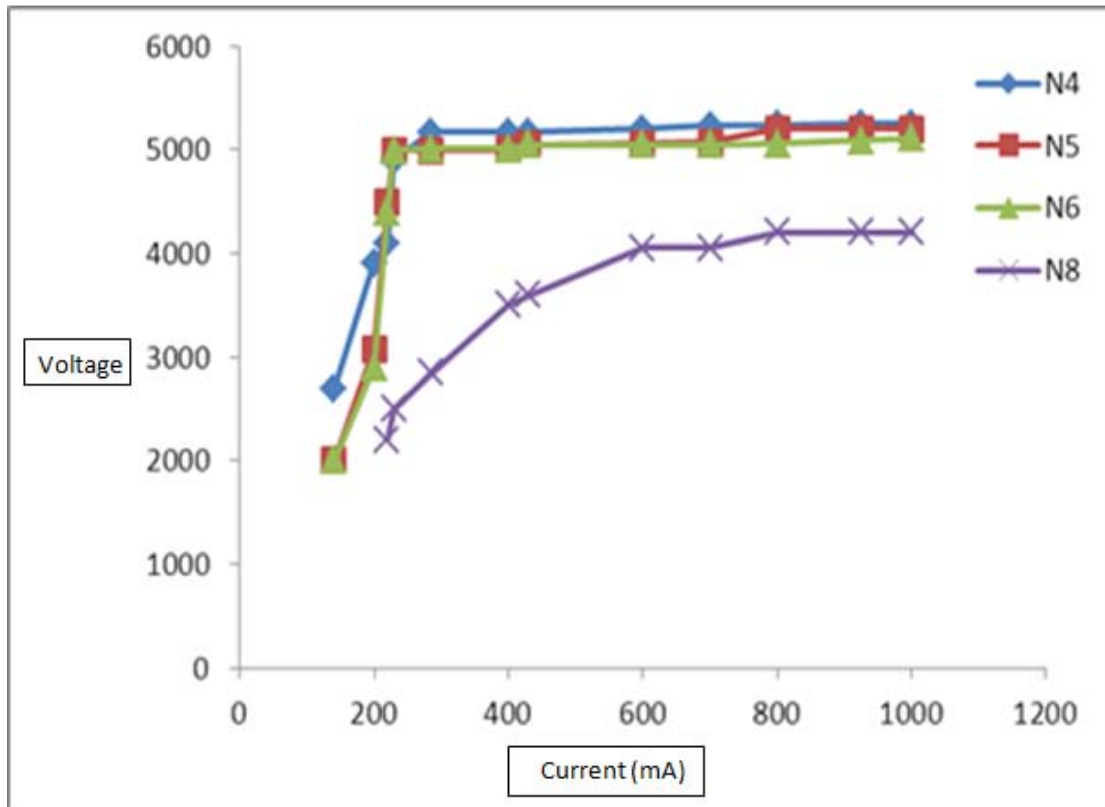


Figure 12: I-V Characteristics of different mixes

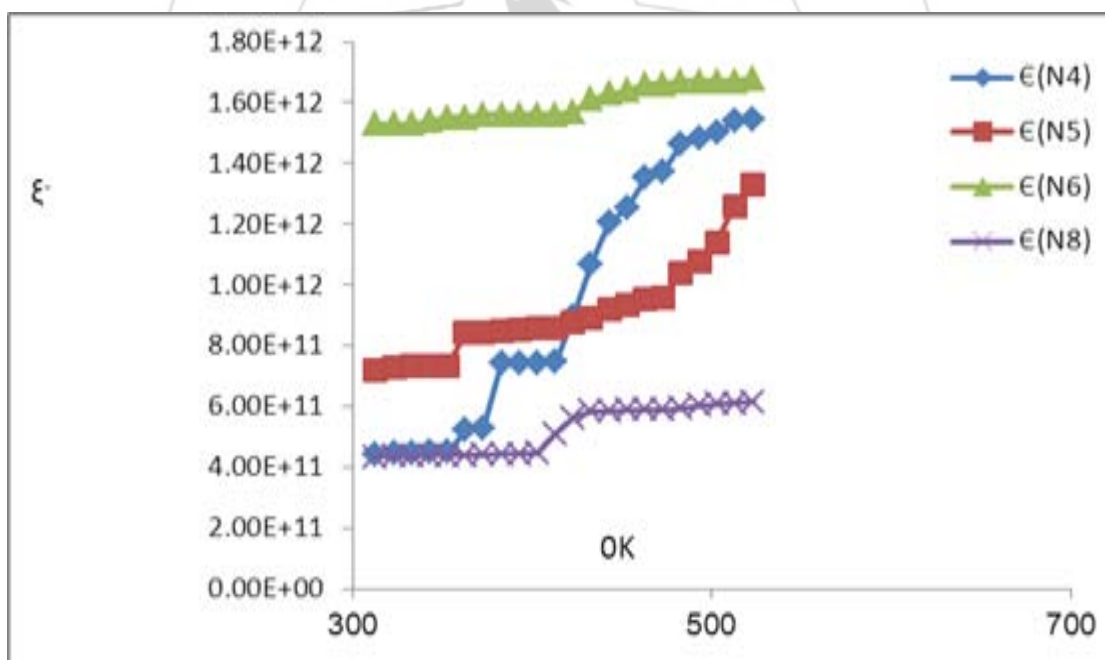


Figure 13: Relation between dielectric constant and temperature OK

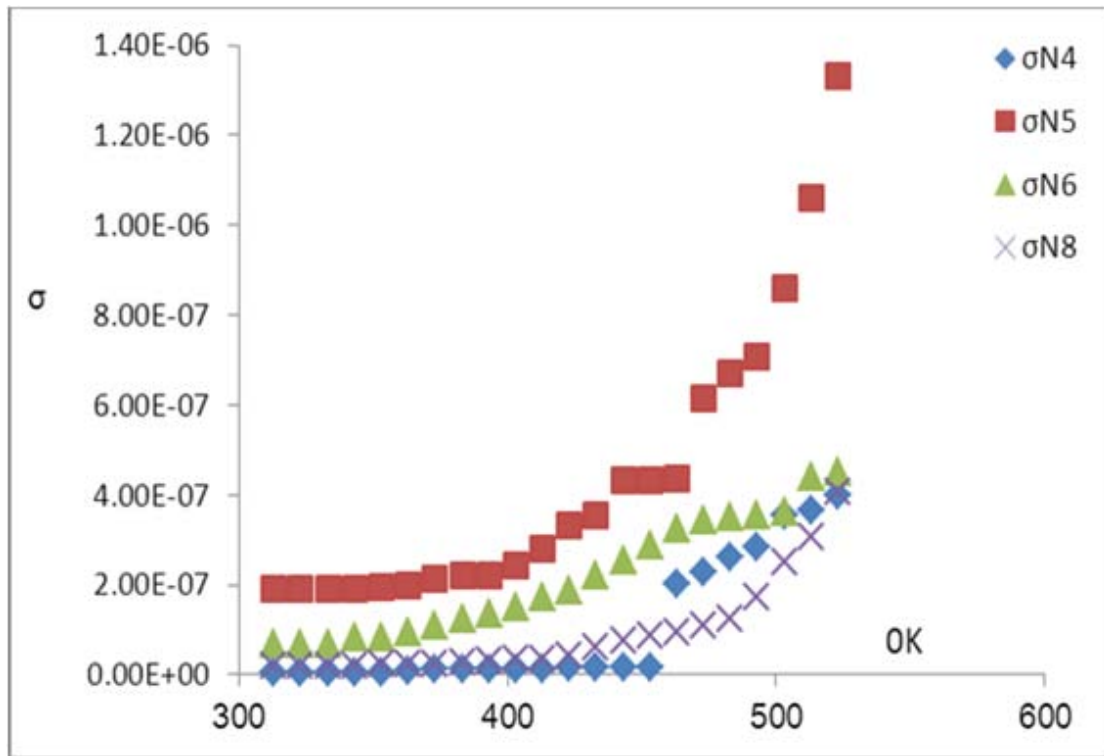


Figure 14: Relation between conductivity and temperature OK

